Structure, Vol. 8, 1069–1077, October, 2000, ©2000 Elsevier Science Ltd. All rights reserved. PII S0969-2126(00)00507-4

Mutual Conformational Adaptations in Antigen and Antibody upon Complex Formation between an Fab and HIV-1 Capsid Protein p24

Stéphanie Monaco-Malbet,*‖ Carmen Berthet-Colominas,* Armelle Novelli,† Nicole Battaï,‡ Nadia Piga,‡ Valérie Cheynet,† François Mallet,† and Stephen Cusack*§

*European Molecular Laboratory Biology
Grenoble Outstation
B.P. 156X
F-38042 Grenoble Cedex 9
France

†Unité Mixte 103 CNRS-bioMérieux
École Normale Supérieure de Lyon
46 allée d'Italie
69364 Lyon Cédex 07
France

‡bioMérieux
Chemin de l'Orme
69820 Marcy l'Étoile
France

Summary

Background: Elucidating the structural basis of antigen-antibody recognition ideally requires a structural comparison of free and complexed components. To this end we have studied a mouse monoclonal antibody, denoted 13B5, raised against p24, the capsid protein of HIV-1. We have previously described the first crystal structure of intact p24 as visualized in the Fab13B5-p24 complex. Here we report the structure of the uncomplexed Fab13B5 at 1.8 Å resolution and analyze the Fab-p24 interface and the conformational changes occurring upon complex formation.

Results: Fab13B5 recognizes a nearly continuous epitope comprising a helix-turn-helix motif in the C-terminal domain of p24. Only 4 complementarity-determining regions (CDRs) are in contact with p24 with most interactions being by the heavy chain. Comparison of the free and complexed Fab reveals that structural changes upon binding are localized to a few side chains of CDR-H1 and -H2 but involve a larger, concerted displacement of CDR-H3. Antigen binding is also associated with an 8° relative rotation of the heavy and light chain variable regions. In p24, small conformational changes localized to the turn between the two helices comprising the epitope result from Fab binding.

Conclusions: The relatively small area of contact between Fab13B5 and p24 may be related to the fact that the epitope is a continuous peptide rather than a more complex protein surface and correlates with a relatively low affinity of antigen and antibody. Despite this, a significant quaternary structural change occurs in the Fab upon complex formation, with additional smaller adaptations of both antigen and antibody.

§To whom correspondence should be addressed (e-mail: cusack@embl-grenoble.fr).

‖Present address: European Synchrotron Radiation Facility (ESRF), BP 220, F-38043 Grenoble Cédex 9, France.

Introduction

High affinity and specific binding of antibodies to foreign antigens is fundamental to the immune response of animals, and extensive structural studies have been undertaken to try to understand this phenomenon. Although there have been numerous Fab structures determined by X-ray diffraction and complexes with haptens or peptides, the number of structures of Fab complexes with protein antigens has risen more slowly. Early work focused on Fab complexes with avian lysozymes [1] and influenza virus neuraminidases [2] but more recently has diversified to include, for example, *E. coli* histidine-containing phosphocarrier protein [3], N10-staphylococcal nuclease [4], influenza virus hemagglutinin [5], human rhinovirus 14 [6,7], human tissue factor [8], and horse cytochrome C [9]. There have been a number of reviews on structural aspects of antibody-antigen association [10–12]. However, there still only exist a few examples, the first being lysozyme [13], in which the structures of the free antibody fragment, free antigen, and the complex are known, permitting a full characterization of the conformational adaptations involved in complex formation.

p24 (or CA) is the major capsid protein of HIV and plays an active structural role both as part of the Gag polyprotein and in its processed form during virus assembly, maturation, and disassembly (reviewed in [14, 15]). It forms a characteristically conically shaped shell surrounding the viral RNA-nucleoprotein complex inside the lipid bilayer of mature virions. Antibodies against p24 are produced early after infection and their detection is widely used as a diagnostic for HIV infection [16]. Although anti-p24 antibodies are not neutralizing, their continued presence in infected patients is correlated with a delayed progression to AIDS. The HIV-1 p24 used in this study is a 243 residue recombinant protein (designated RH24, derived from HIV-1 strain HXB2) with an N-terminal extension containing a His_6 tag and also a slightly modified C terminus [17, 18]. 13B5 is a mouse $IgG1_\kappa$ monoclonal antibody raised against RH24 [18].

Here we report the 1.8 Å resolution crystal structure of the free Fab′13B5 and compare it to the 3 Å resolution structure of the antigen-bound Fab13B5 [18]. We also analyze the modifications of the antigen structure due to binding by comparing the complex structure to that of the free C-terminal domain of p24 [19]. This enables us to highlight the various induced fit interactions in both antigen and antibody that occur during complex formation.

Results and Discussion

As described in the Experimental Procedures, we have determined the cDNA nucleotide sequence of the light and heavy chains of 13B5 Fab and report in Figure 1 the corresponding amino acid sequences. The uncomplexed structure is of the Fab′13B5 (obtained by pepsin cleavage), whereas in the p24 complex crystals, the Fab was used (obtained by papaïn cleavage). As the slightly different Fab heavy chain length in each case is unlikely to have a direct impact on the binding interface, for clarity, we use the term Fab for both the molecule found in the complex as well as the free Fab′. In the following, the Fab will

Key words: antigen; antibody; Fab; HIV-1; p24; CA; protein-protein interactions; X-ray crystallography

Fab13B5_H:

```
          10        20                  40        50
EVQLQQSGAELARPGASVKMSCKASGYTFTSYTMHWVKQRPGQGLEWIGY
          60        70        80        90        100
INPSSGYSNYNQKFKDKATLTADKSSSTAYMQLSSLTSEDSAVYYCSRPV
          110       120       130       140       150
VRLGYNFDYWGQGSTLTVSSAKTTPPSVYPLAPGSAAQTNSMVTLGCLVK
          160       170       180       190       200
GYFPEPVTVTWNSGSLSSGVHTFPAVLQSDLYTLSSSVTVPSSTWPSETV
          210
TCNVAHPASSTKVDKKIVP
```

Fab13B5_L:

```
          10        20                  40        50
EIVLTQSPAITAASLGQKVTITCSASSSVSYMHWYQQKSGTSPKPWIYEI
          60        70        80                  100
SKLASGVPARFSGSGSGTSYSLTISSMEAEDAAIYYCQQWNYPFTFGSGT
          110       120       130       140       150
KLEIKRADAAPTVSIFPPSSEQLTSGGASVVCFLNNFYPKDINVKWKIDG
          160       170       180       190       200
SERQNGVLNSWTDQDSKDSTYSMSSTLTLTKDEYERHNSYTCEATHKTST

SPIVKSFNRNEC
```

Figure 1. Amino Acid Sequences of the Heavy and Light Chains of Fab13B5

The CDRs, according to Kabat's [20], are surrounded with rectangles. Nucleotides corresponding to the last four residues of the light chain (in italics) were not sequenced due to choice of primer and are assumed to be RNEC as in other light chains. Electron density for Arg-209 and Asn-210 are observed in the crystal structure.

be numbered sequentially, with matching Kabat [20] numbers provided in square brackets.

The association and dissociation rates and affinity constant for the formation of the 13B5 Fab complex with RH24 have been determined by surface plasmon resonance measurements (see Experimental Procedures). An association rate of 3.5×10^5 $M^{-1}s^{-1}$ and a dissociation rate of 1.2×10^{-3} s^{-1} were derived corresponding to an affinity of 29 nM. This value is in the lower range for antibody-antigen complexes principally due to the fast dissociation rate.

Overall Structure and Quality of the Models

The structure of the Fab13B5 was solved by molecular replacement and refined at 1.8 Å resolution to an R factor of 22.5% and R free of 25.5%. It consists of residues H1 to H219 [H1–H212] and L1 to L210 [L1–L212] of the heavy chain and light chain, respectively. Fab13B5 is a typical Fab with the immunoglobulin fold for each of its domains (Figure 2). All disulphide bridges are visible, although the bridge between L132–L192 [L134–L194] is partially broken. Most of the residues are in energetically favorable (90.1%) or allowed (99.2%) regions of the Ramachandran plot. As found in other Fab structures (e.g., [8]), Ile-L50 [L51] of the light chain is located in an unfavorable region of the Ramachandran plot: it lies in the (i + 1) position of a classic γ turn [21]. Nine residues belonging to two loops exposed to solvent in the constant domains (L154→L156 and H135→H140) have poor electron density. Multiple rotamers, particularly for serines and valines, are visible in the solvent-exposed regions (17 in the light chain and 3 in the heavy chain). The elbow angle of Fab13B5 is 151.4°, which is in the middle range of elbow angles [22]. The conformations of the CDR loops L1, L2, H1, and H2 are consistent with their sequence-predicted canonical structure types [23], which are type 1, 1, 1, and 2, respectively. L3 of type 3 is less well structurally predicted than the other CDRs because of a Phe-L94[L96] instead of a Pro at this position.

The 3 Å resolution structure of the Fab13B5-RH24 complex (Figure 2), solved by molecular replacement using the Fab13B5 structure, was refined to an R factor of 21.6% and R free of 28.2% [18]. The antigen-bound Fab13B5 consists of the same residues as for the free Fab13B5, with regions L152-L155 and H134–140 again poorly ordered. The model of p24 starts at residue P13 and ends at residue P220 (p24 numbering), with the first 27 amino acids, including the His-tag and the last 8 residues of RH24, missing. p24 is composed of flexibly linked N-terminal and C-terminal helical domains (Figure 2). We have recently found that the structure of the Fab13B5-p24 complex is essentially unchanged when, instead of RH24, a p24 construct with a mature N terminus (Pro-1) and a C-terminal extension (the p2 or SP1 peptide) is used (C. B.-C., H.-G. K., and S. C., unpublished data). The only significant difference is that, in this case, the N-terminal of p24 is ordered and forms a hairpin structure with Pro-1 buried and interacting with Asp-51 as previously described [24]. The p2 peptide is disordered, as also reported in a structure of a similar p24 construct [25].

Antigen Binding Site

The continuous epitope recognized by 13B5 comprises helix H10–turn–helix H11 of the C-terminal domain of p24. Figure 3 illustrates the good shape complementarity of the surfaces of the paratope and its epitope. The surface area buried in the antigen-antibody interface, calculated with a 1.7 Å probe using the CCP4 program SURFACE, is 609 $Å^2$ for the antibody and 750 $Å^2$ for p24. This buried surface is on the low side for protein-Fab complexes according to the compilation of Huang et al. [8]; this study, however, used a different program (MS) for the surface calculation, giving systematically lower results than calculations using SURFACE. The heavy chain accounts for 82% of the total antibody-antigen contact surface, whereas the light chain only contributes 18% (Figures 4a and 4b). The domination of the heavy chain is normally found in antigen-antibody complexes [8, 11] but is extreme here due to the fact that CDR-L1 and CDR-L2 do not contribute directly to the interaction at all. Of the four CDRs of the Fab that directly participate in the antigen interaction, CDR-L3, CDR-H1, CDR-H2, and CDR-H3 contribute 18%, 14%, 33%, and 33% of the buried surface, respectively. Although the contributions of CDR-L1 and L2 to antigen contacts are generally lower than the other CDRs [11], complete absence of contact to both is more characteristic of Fab complexes with hapten or peptide rather than protein antigens [8,11].

Table 1 summarizes the residues in contact at the Fab13B5-RH24 interface. A total of 11 p24 residues participate in the interface and 14 amino acids of Fab13B5 make contacts with the antigen (Figure 4c). The epitope is almost continuous and includes residues 204-ALGPAAT(L)EE(MM)TA-217; those not contacted are in brackets. This is fully consistent with the binding region 203-KALGPAATLEEMMTA-217 identified by immunoscreening a library of bacterial clones, each expressing a peptide derived from RH24 (data not shown). The antibody combining site consists of contacting residues Trp-90[Trp-91], Asn91 [Asn-92], Tyr-92[Tyr-93], Phe94[Phe96] (CDR-L3), Thr-30 (framework-H1), Ser-31[Ser-31], Tyr-32[Tyr-32], Thr-33[Thr-33] (CDR-H1), Tyr-50[Tyr-50], Asn-52[Asn-52], Tyr-57[Tyr-56], Asn-59[Asn-58] (CDR-H2), Val-101[Val-98], and Tyr105[Tyr100A] (CDR-H3). The resolution of the complex (3 Å) does not allow us to see water molecules either in the interface or close to it. The greater impor-

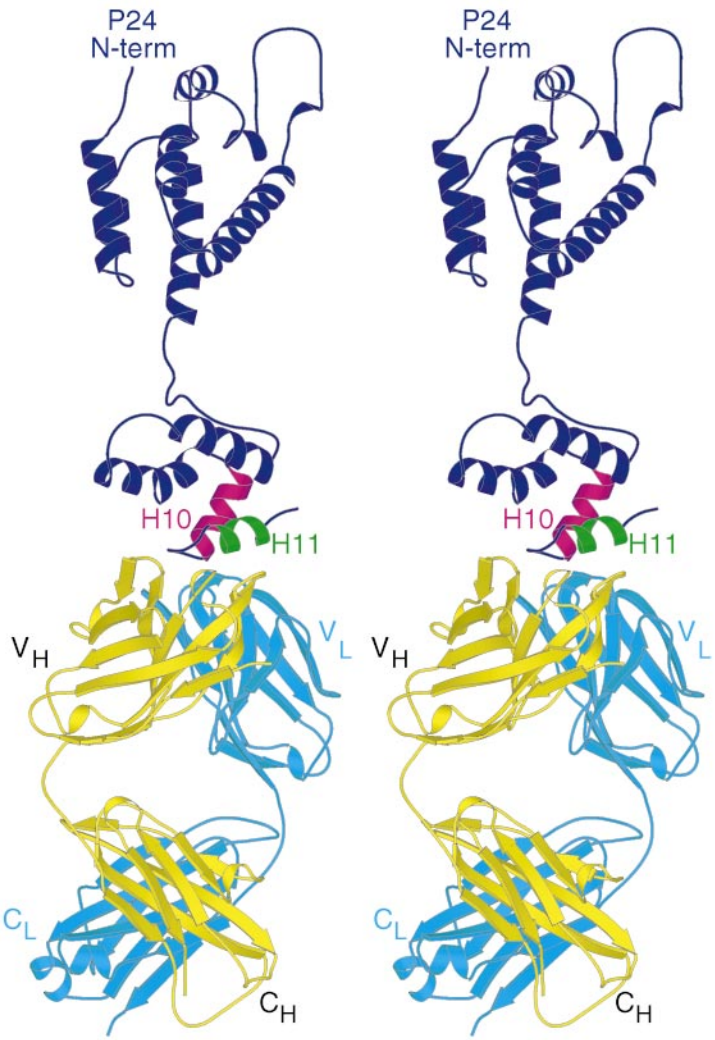

Figure 2. Stereographic Ribbon Representation of the Fab13B5-p24 Complex

p24 is colored in blue, with H10 and H11 taking part of the interaction with the Fab and depicted, respectively, in magenta and green. The light chain of the Fab13B5 is colored in cyan while its heavy chain is in yellow.

tance of the heavy chain compared to the light chain in binding the epitope is confirmed by the analysis of the detailed interactions (Table 1). Of the 75 van der Waals contacts observed, 65 involve atoms of the heavy chain, and of 8 hydrogen bonds between Fab and p24, 7 are made to heavy chain residues. CDR-H2 is particularly strongly involved in interactions at the antigen-antibody interface. Half of the residues involved in the interaction with the antigen are aromatic, and the majority of them are tyrosines. The importance of aromatic residues as antigen-contacting residues has already been observed in many antibody-antigen complexes [13].

Conformational Changes of the Fab upon Binding

Quaternary Changes

The elbow angle of the Fab complexed with RH24 has been calculated from three distinct complexes: crystal type I with 2 complexes per asymmetric unit and crystal type II with one complex per asymmetric unit [18]. The results are 148.7° and 152.4° for type I crystals and 151.0° for type II; these should be compared to 151.4° for the unbound Fab. These results show that the elbow angle does not change significantly upon antigen binding: the small variations observed are possibly due to crystal packing. On the other hand, there is a significant change in the relative orientation of the variable domains between the antigen-bound and unbound states (Figures 5a and 5b). After superimposing the VL domains of each state, an additional rotation of 8.3° is required to bring the VH domains into optimal coincidence (8.3° and 8.1° for complex type I crystals and 8.3° for type II crystals). This is not the largest such movement observed in an Fab upon antigen binding (e.g., 16.3° between VH and VL in an HIV-1 neutralizing antibody Fab 50.1 [26]) but it belongs to the higher range [11]. The surface of VH occluded upon interaction with VL varies between 840 Å^2 and 865 Å^2 in the complexed forms of the Fab and is 865 Å^2 in the unbound form. The buried surface of VL through its interaction with VH varies between 895 Å^2 and 940 Å^2, while it is 950 Å^2 in the free Fab. On this basis we conclude that the strength of the VH:VL interaction is not significantly modified by the relative movement of the two domains.

Tertiary Changes

To determine whether any tertiary conformational changes accompany antigen binding, each variable domain of the free Fab (VL and VH) was superimposed individually on the corresponding ones of the complexed Fab (type II crystals) using the Cα positions of the framework residues. The root-mean-square deviation (rmsd) calculated over all Cα positions of the VH domain between

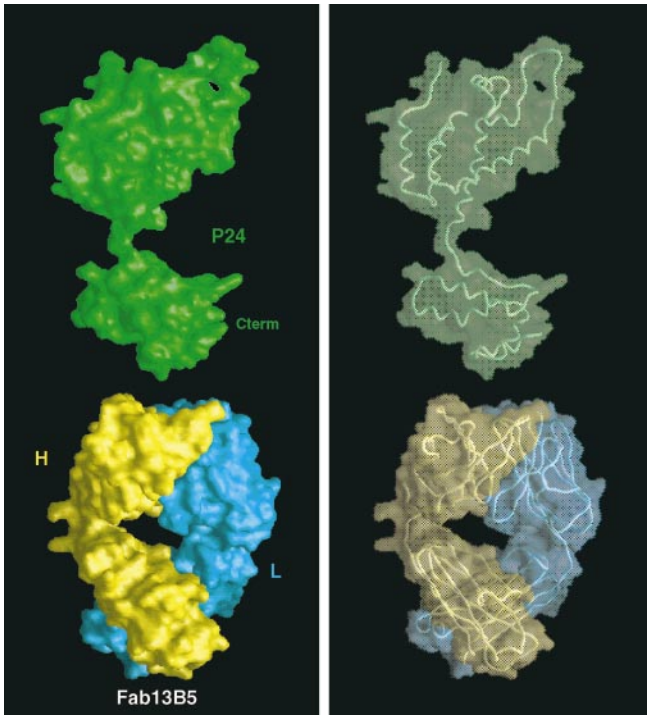

Figure 3. Solid and Transparent Surface Representations of the Complex Fab-p24

The p24 molecule is translated away from the interaction surface to allow a clearer view of the binding interface.

the free and bound states of the Fab is 0.8 Å compared to 0.25 Å for the VL Cα positions. This suggests that the more significant structural changes induced by the binding are localized to the VH domain, consistent with the much greater involvement of this domain in epitope binding.

Examination of the VL domain shows that CDR-L3 of the free Fab (Trp-L90, Asn-L91, Tyr-L92, Pro-L93) makes a crystal contact with the CL domain of one of its symmetry-related molecules (Glu-L185, Arg-L186, Asn-L188, Arg-L209, Asn-L210). Although the contacts are quite different from those observed in the complex structure, the residues of the Fab involved in the binding to the epitope have very similar conformations in both structures. The hydrogen bond observed in the complex between the main chains of Tyr-L92(N) and Ala-P204(O) is mimicked in the free Fab structure by a water molecule placed exactly at the position corresponding to Ala-P204(O).

The most significant deviations between complexed and uncomplexed Fab concern the region H99 to H108 of CDR-H3, where the rmsd over all atoms is 1.8 Å. In fact, CDR-H3 moves away from the VH domain as if it was more rigidly fixed to the VL domain during the binding-induced relative rotation of VH and VL. This is understandable, as analysis of the VH:VL interaction shows that half of it is made by the CDR-H3 of VH. An important consequence of the relative movement of CDR-H3 is that it permits the antigen (particularly Glu-P213) to penetrate more deeply between CDR-H3 and CDR-H1 (Figure 5a).

Apart from CDR-H3, local changes are small or are less easy to interpret due to crystal contacts. The CDR-H1 residues do not change their relative position to the VH domain upon binding (overall atom rmsd of 0.3 Å). The two hydrogen bonds observed in the p24 complex interface are again mimicked in the free Fab structure by two water molecules. The side chain of Tyr-H50 makes a near 90° rotation around its Cβ-Cγ bond upon antigen binding, permitting it to form the hydrogen bond [Tyr-H50(OH) and Ala-P208(N)] observed in the complex structure. However, such a rotamer would be disallowed in the crystals of the free Fab, as it would cause a bad contact with Asp-L149 of a symmetry-related molecule. It is therefore difficult to assign from this data the movement of the Tyr-H50 side chain only to the binding of the epitope. The same problem arises with Asn-H52, which makes a hydrogen bond with the main chain oxygen of Ala-P208 in the complex and a van der Waals contact with Asp-L149 of a symmetry-related molecule in the free Fab crystal. In both cases, the conformation of this amino acid in the other structure would make a bad crystal contact. The observed movement of Ser-H54 between the free and bound states of the Fab is correlated with the movement of Asn-H52 described above.

Conformational Changes of the Epitope upon Binding

We have compared the structure of the p24 epitope in the Fab13B5 complex with that of the free C-terminal domain of p24 (strain NL43) determined to 1.7 Å (Protein Data Bank entry 1AM3, [19]). The two p24 proteins are derived from different HIV-1 subtype B strains and differ by one mutation in the epitope: in RH24 (derived from strain HXB2), Ala-208 is replaced by Gly-208 in NL43. We have found that a p24 with Gly-208 has slightly reduced affinity for Fab13B5, but the Fab-p24 complex still crystallizes to give a very similar crystal form to that obtained with RH24 (C. B.-C., H.-G. K., and S. C., unpublished data). It should also be pointed out that in the 1AM3 crystal structure the epitope is in contact with two symmetry related molecules.

The only significant difference observed in the Ala-204 to Ala-217 region between the free and complexed structures is localized around Pro-207 and Ala-208, which belong to the turn between helix 10 and helix 11 (Figure 6). The largest atomic displacement observed is 4 Å and corresponds to the carbonyl oxygen of Pro-207 which is pointing in opposite directions in the two structures. The turn is flexible and adapts to the contacts in which it is involved with its neighbors. In the 1AM3 structure, the main chain of Pro-207 makes a hydrogen bond with the side chain of Arg-173 of a symmetry-related molecule. In the Fab-complex structure, Pro-207 is not involved in hydrogen bonding but is in van der Waals contacts with the Fab13B5. The following residue, Ala-208, makes two main chain hydrogen bonds with residues of the CDR-H2 of the Fab (Tyr-H50 and Asn-H52). Due to the mutation and the crystal contact in the 1AM3 structure, it is therefore difficult to attribute conclusively the differences in the two structures to the binding of the Fab. However, the crystal contacts observed in the 1AM3 structure are less extensive than those found in the complex structure. It is therefore reasonable to imagine that the uncomplexed state of p24 in this region is close to the 1AM3 structure and that the observed movement is due to binding to the Fab, this new arrangement being stabilized by two additional hydrogen bonds. It would be desirable to validate this conclusion with a structure of the C-terminal domain, which does not have crystal contacts in this area and has an alanine in position 208. Ala-208 can have the same configuration as Gly-208, since Gly208 in 1AM3 belongs to a favorable region of the Ramachandran plot. On the other hand, as mentioned above, we have determined a 3.3 Å structure of a p24(Gly-208)-Fab13B5 complex. This structure shows that the mutation Ala→Gly-208 leads to no observable perturbation of the Fab-epitope interface apart from removal of the methyl group (C. B.-C., H.-G. K., and S. C., unpublished data).

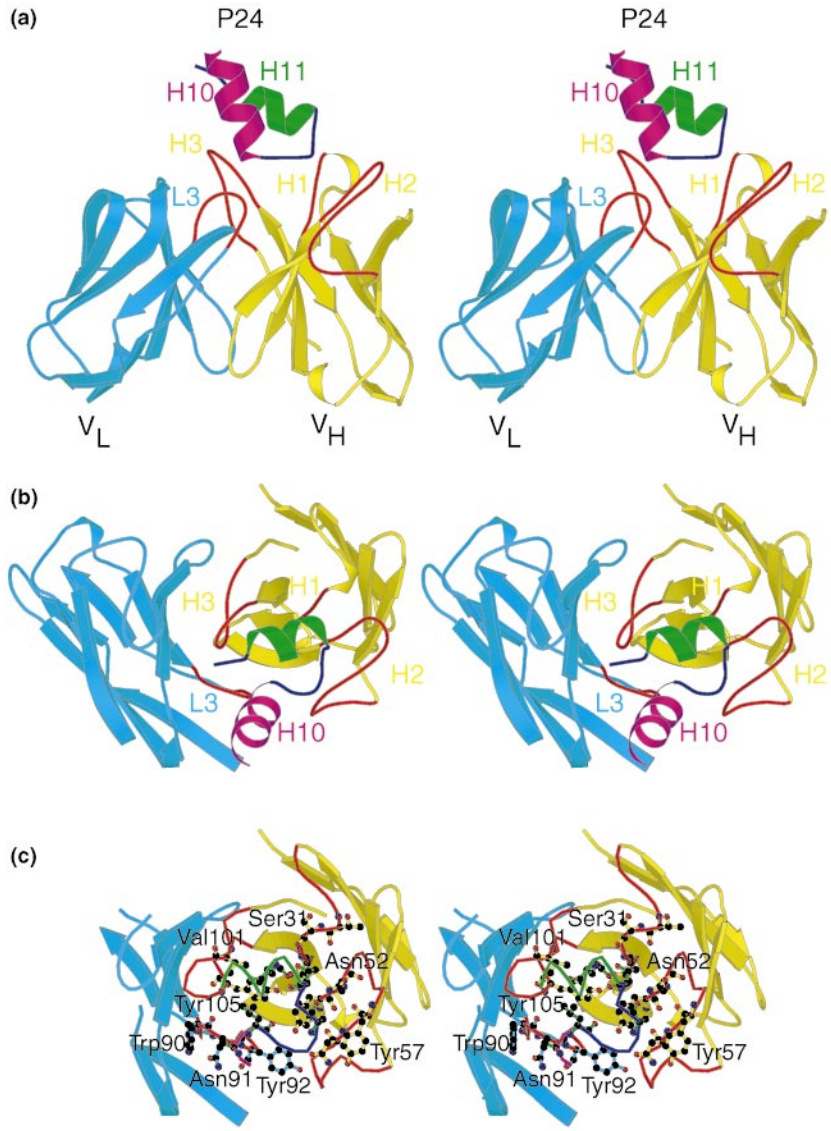

Figure 4. (a) Stereographic Representation of the Variable Domains of the Fab Bound to the p24 Epitope

(a and b) Two views at 90 degrees. The CDRs of the Fab involved in the binding are colored red and labeled H1, H2, H3, and L3 for CDR-H1, CDR-H2, CDR-H3, and CDR-L3.

(c) As (b) but with full side chains of the amino acids involved in hydrogen bonds and some residues involved in van der Waals contacts between Fab and p24 shown. Some regions of the light chain have been truncated for clarity.

Biological Implications

In this study we examined the effect of the binding of p24, the capsid protein of HIV-1, to a fragment of a monoclonal antibody (Fab13B5) recognizing its C-terminal domain on the structure of both the Fab and the antigen. The structure of the complex Fab-p24 was solved and described recently to 3 Å resolution [18]. We report here the structural determination of the Fab13B5 alone to 1.8 Å. We also analyze the structural changes observed between the Fab bound to p24 and the "free Fab" as well as p24 bound to the Fab and the "free p24" [19].

In terms of buried surface area, the antigen binding site is rather small compared with what is described in the literature for a typical antigen of 25 kDa. It involves only 4 CDRs (H1, H2, H3, L1) out of 6, which is unusual for a protein antigen, with a major contribution of the heavy chain (82% of the surface area) observed also at the level of individual amino acid interactions. Half of the amino acids of the Fab involved in the interaction with the antigen are aromatic, and the majority of them are tyrosines.

The comparison of the free Fab structure with that in the p24 complex allows an analysis of the adaptation of the Fab variable domain, and we find structural adjustments at various levels. At the quaternary level, a large relative rotation of 8° between the variable regions of light and heavy chains is observed while preserving a similar area of contact between the two chains. There is also a concerted movement comprising CDR-H3 (H99-H108), which remains rigidly attached to the VL domain rather than the VH domain and which allows the epitope to penetrate deeper into the Fab surface. At the more local level, side chain movements are essentially located in the VH domain. A similar analysis for the p24 epitope, which comprises a helix-turn-helix motif, is possible using the structure of the isolated p24 C-terminal [19]. Although crystal contacts and a point mutation in the epitope in the isolated p24 C-terminal domain structure complicate the interpretation, it appears likely that Fab binding induces a structural change in the turn between helix 10 and helix 11, centered on Pro-207. The new structure is stabilized by two hydrogen bonds to the Fab.

The relatively low measured affinity of the Fab for RH24 (29nM) is perhaps correlated with two aspects of the structure described here. First is the relatively small area of contact between Fab and

Table 1. Interactions Observed between Fab13B5 and RH24 in the Complex

	Fab13B5-L								Fab13B5-H					
	CDR-L3				CDR-H1				CDR-H2				CDR-H3	
RH24	W90 [W91]	N91 [N92]	Y92 [Y93]	F94 [F96]	T30 [T30]	S31 [S31]	Y32 [Y32]	T33 [T33]	Y50 [Y50]	N52 [N52]	Y57 [Y56]	N59 [N58]	V101 [V98]	Y105 [Y100A]
A204	1V	6V	H-1V	2V	–	–	–	–	–	–	–	–	–	–
L205	–	–	–	1V	–	–	–	–	H-1V					3V
G206	–	–	–	–	–	–	–	–	3V	–	–	–	–	–
P207	–	–	–	–	–	–	–	–	2V	–	4V	1V	–	–
A208	–	–	–	–	–	–	–	1V	H-7V	H-3V	2V	–	–	–
A209	–	–	–	–	–	–	–	–	–	2V	–	–	–	–
T210	–	–	–	–	1V	H-3V	–	–	–	6V	–	–	–	–
E212	–	–	–	–	–	3V	–	–	–	–	–	–	–	–
E213	–	–	–	–	–	1V	1V	H-6V	–	–	–	–	3V	2H-6V
T216	–	–	–	–	–	–	–	–	–	–	–	–	1V	–
A217	–	–	–	–	–	–	–	–	–	–	–	–	3V	–

The Fab numbering follows its true sequence and the corresponding Kabat numbering [20] is indicated in brackets. The van der Waals contacts are represented by a V preceded by the number of such contacts (≤ 4 Å). Hydrogen bonds (≤ 3.3 Å) are indicated with an H.

antigen, which more closely resembles a Fab-peptide complex. Second is the mutually induced fit mode of recognition, which may involve an extra cost in energy or entropy that offsets the binding energy.

These results provide further evidence for the subtlety of specific antigen-antibody recognition involving both global and local adaptations of the Fab structure.

Experimental Procedures

Sequencing of the Fab13B5

mRNA was extracted from 13B5-producing hybridoma cells, reverse transcribed, and then amplified by polymerase chain reaction (PCR) using oligonucleotides specific for IgG1κ immunoglobulin heavy and light chain DNA sequences. N-terminal microsequencing of the light chain helped to design more precisely the corresponding primer (the N-terminal of the heavy chain was found to be blocked). The PCR products were cloned into a pUAg vector (The Ligator, R&D systems). Five clones for each chain were totally sequenced (both strands) on a Perkin Elmer 377 automated sequencer. The resultant amino acid sequences of the light and heavy chains of Fab13B5 are given in Figure 1.

Protein Purification

Murine monoclonal antibodies 13B5 (subclass IgG1κ) were raised against the recombinant HIV-1 capsid protein (RH24). The antibodies were purified from ascitic fluid on a protein A Sepharose 4FF affinity column (Pharmacia). Dimeric Fab'_2 fragments were generated by pepsin digestion (pepsin aga-

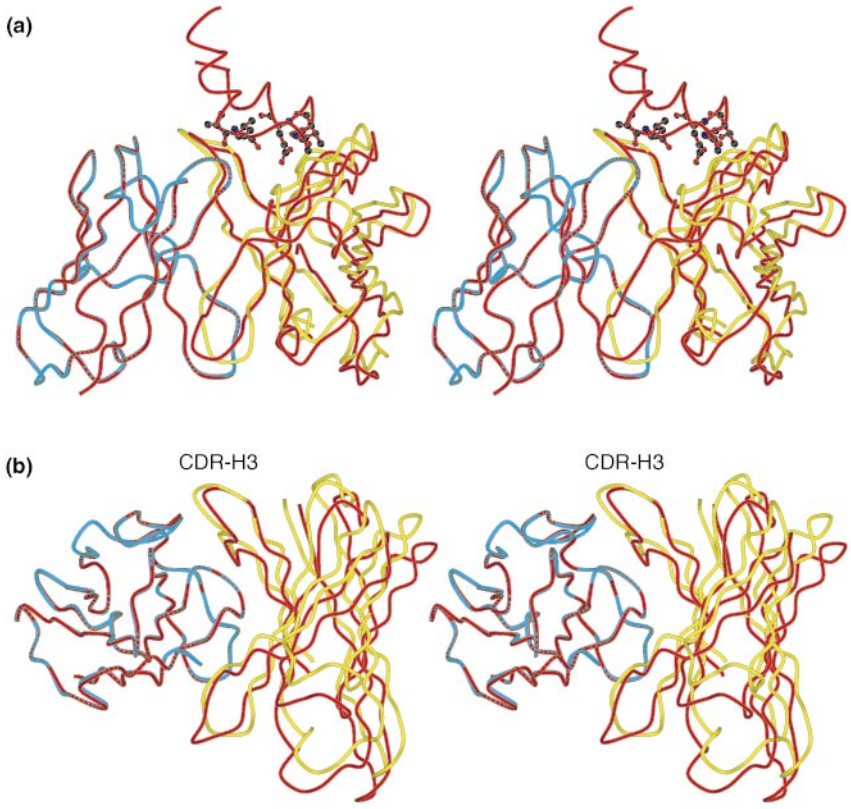

Figure 5. Superposition of the Free and Complexed Structures of the Fab13B5 via Their VL Domains

The free Fab13B5 is colored in yellow (VH) and in cyan (VL), while the bound Fab complexed to the C-terminal domain of the antigen is colored in red. (a) and (b) are two views of the structure differing by a rotation of 90 degrees.

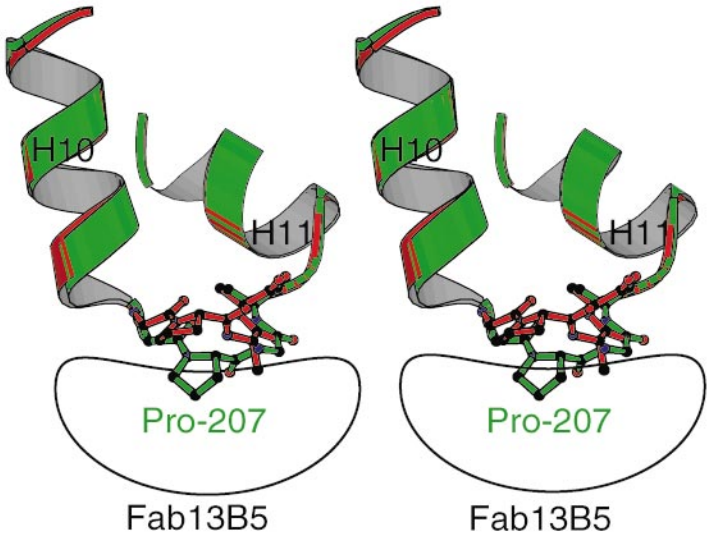

Figure 6. Adaptation of the p24 Epitope upon Fab Binding

The C-terminal domain of p24 in the epitope region (H10-turn-H11) as in the Fab complex (red) is superposed on the isolated C-terminal domain of p24 (green; Protein Data Bank entry 1AM3, [19]), showing conformational differences at Pro-207.

rose, Sigma, ref. P3286) at 37°C at pH 3.5, which was stopped by addition of bicarbonate to pH 7.0. The Fab′$_2$ were then incubated at 37°C in presence of β-mercaptoethanol (30 mM final) and the reaction stopped on ice. The resulting monomeric Fab′13B5 was concentrated to 7 mg/ml in a sodium phosphate buffer of 10 mM at pH 6.0 in presence of 5 mM EDTA. Preparation of Fab13B5 and RH24, Fab-antigen complex formation, crystallization, and structure determination of the Fab13B5-RH24 complex are described elsewhere [18].

Determination of the Kinetic Constants of the 13B5–RH24 Complex

The binding of mAb 13B5 to RH24 was measured by BIAcore analysis with the Fab form of the mAb to avoid the experimental and computational problems associated with the use of bidendate ligands [27, 28]. All experiments were performed on a BIAcore 1000 instrument (Pharmacia Biosensor) according to the manufacturer's instructions. HEPES-buffered saline (10 mM HEPES [pH 7.4], 150 mM NaCl, 3.4 mM EDTA, 0.05% surfactant P20 [Pharmacia]) was used as the running buffer at a flow rate of 5 μl/min. RH24 recombinant protein (1 μg/ml in 10 mM acetate buffer [pH 5.0]) was immobilized via the primary amine groups as described previously [29, 30] using N-hydroxysuccinimide/N-ethyl-N' (3-dimethylaminopropyl) carbodiimide coupling reagents to a final resonance value of 100–500 resonance units. Fab13B5 was diluted to 2.38–119 nM in HEPES-buffered saline and injected at a flow rate of 20 μl/min. The association and dissociation rates of the mAb was determined using BIAevaluation 2.1 software (Pharmacia BIAsensor) and a homogeneous 1:1 model, according to methods described previously [27, 28].

Crystallization and Data Collection

Two microliters of Fab′13B5 were mixed with 2 μl of precipitant solution and allowed to equilibrate in hanging drops at 22°C over 1 ml of precipitant solution (9%–11% PEG8000 in 0.1 M PIPES buffer at [pH 7.8]) for a minimum of 10 days. For data collections, crystals of an average size of 300 μm × 150 μm × 80μm were soaked stepwise in PEG400 to 30%, fished in a

Table 2. X-Ray Diffraction Data for Crystals of the Fab′13B5

Experimental Conditions	
X-ray source	BM14 (ESRF)
Wavelength (Å)	0.799
Sample temperature	100K
Crystal Parameters	
Resolution (Å)	15–1.8
Unit cell (Å)	36.7 81.7 134.2
Space Group	$P2_12_12_1$
Mosaïcity	0.9
Percent solvent	44%
Data Processing	
Number reflections used	124392
Number unique reflections	35964
Intensity > 3σ (%)	93.6 [84.3][a]
Completeness (%)	94 [85.5][a]
R_{sym} (%)	6.3 [12.8][a]

[a]Values in brackets correspond to outer shell resolution.

Table 3. Refinement Statistics for the Fab′13B5 Structure

Refinement parameters	
Resolution (Å)	15-1.8
Number of protein atoms	3277
Number of water molecules	237
Number of work reflections	31917
Number of free reflections	3532
R Factors (%)	
R	0.225
R_{free}	0.255
<B> Average Atomic Temperature Factors (Å^2)	
<B> Protein	25.8
<B> Side chains	28.1
<B> Main chain	25.8
<B> Solvent	34.4
Rms Deviations from Ideal Geometry	
Bonds (Å)	0.005
Angles (°)	1.4
Ramachandran Plot	
Favourable (%)	90.4
Additional (%)	9.1
Generous (%)	0.3
Forbidden (%)	0.3 (Ile L50)

The disordered residues L154 to L156 and H135 to H140 are excluded from the evaluation of the statistics.

mounted cryoloop, and flash frozen to 100 K. They belong to the space group $P2_12_12_1$ with unit cell dimensions of a = 36.7 Å, b = 81.7Å, and c = 134.2 Å. The Matthews coefficient [31] Vm is 2.2 Å^3/Da, with one molecule in the asymmetric unit corresponding to a solvent content of 44%. A low resolution (3 Å) and a high resolution (1.8 Å) data set were collected on the bending magnet beamline BM14 at the ESRF (wavelength = 0.799 Å) from a single frozen crystal. The data were processed using MOSFLM [32], and the data scaling and reduction was carried out with the CCP4 package [33] (Table 2).

Structure Determination and Refinement

The Fab crystal structure was solved by molecular replacement using AMoRe [34]. The Fab 25.3 from the Fab 25.3-p24 complex (Protein Data Bank entry 1AFV, [35]) was used as the search model. The sequence identity of the heavy and light chains of the two Fabs is, respectively, 86.3% and 81.9%. The whole model gave a straightforward solution with a correlation coefficient after fitting in AMoRe of 0.537 against 0.303 for the next solution. The same solution was found by separately searching for the constant dimer (CL:CH1) and the variable dimer (VL:VH). The XPLOR package was used to refine the Fab′13B5 model using the slow cooling protocol [36] and other standard protocols. Several cycles of refinement and model building were carried out using O [37] and a combination of 2Fo-Fc, Fo-Fc, and omit maps, to a final R factor of 22.5% and R free of 25.5% (calculated with 10% of the data not used in the refinement). Table 3 summarizes the refinement statistics.

Analysis of the Structures

The quality of the model was verified by PROCHECK [39]. Buried surface areas were calculated with the program SURFACE (CCP4) with a 1.7 Å probe radius and water molecules excluded from the calculation. Hydrogen bonds ($\leq$ 3.3 Å) and van der Waals contacts ($\leq$ 4 Å) between the Fab and its antigen were found by the program CONTACT (CCP4) and visualized with the program O [37]. Superposition of Fab domains and rmsd calculations were performed using the program LSQMAN [38]. Framework residues chosen for superposition of VH to VL and CH1 to CL were taken from the structural alignment proposed by Padlan [22]. To evaluate the relative movement of the variable domains upon binding, VL domains of the free and complexed Fab were first superimposed based upon the Cα positions. The relative rotation of the corresponding VH domains was then determined by subsequent mapping of the Cα positions of their framework residues.

Acknowledgments

We are very grateful to Christine Hébrard and Michèle Guillote (bioMérieux) for technical help and discussions on p24 preparation and the Fab-p24 affinity measurements. We also thank Michel Arnaud (bioMérieux) for advice concerning the Fab sequencing and Geneviève Sibaï for preparation of the Fab. We finally thank Andy Thompson (EMBL) for assistance with BM14 measurements on the Fab and Wim Burmeister (ESRF) for assistance on ID14-EH3 for the measurements on RH24-Fab. Hans-George Kräusslich and Ingolf Gross provided purified p24 and p24-p2 protein.

Received: June 6, 2000
Revised: August 25, 2000
Accepted: September 5, 2000

References

1. Braden, B.C., et al., and Poljak, R.J. (1994). Three-dimensional structures of the free and the antigen-complexed Fab from monoclonal antilysozyme antibody D44.1. J. Mol. Biol. *243*, 767–781.
2. Malby, R.L., et al., and Colman, P.M. (1994). The structure of a complex between the NC10 antibody and influenza virus neuraminidase and comparison with the overlapping binding site of the NC41 antibody. Structure *2*, 733–746.
3. Prasad, L., et al., and Delbaere, L.T. (1993). Evaluation of mutagenesis for epitope mapping. Structure of an antibody-protein antigen complex. J. Biol. Chem. *25*, 10705–10708.
4. Bossart-Whitaker, P., Chang, C.Y., Novotny, J., Benjamin, D.C., and Sheriff, S. (1995). The crystal structure of the antibody N10-staphylococcal nuclease complex at 2.9 Å resolution. J. Mol. Biol. *253*, 559–575.
5. Bizebard, T., et al., and Knossow, M. (1995). Structure of influenza virus haemagglutinin complexed with a neutralizing antibody. Nature *376*, 92–94.
6. Smith, T.J., Chase, E.S., Schmidt, T.J., Olson, N.H., and Baker, T.S. (1996). Neutralizing antibody to human rhinovirus 14 penetrates the receptor-binding canyon. Nature *383*, 350–354.
7. Che, Z., et al., and Smith, T.J. (1998). Antibody-mediated neutralization of human rhinovirus 14 explored by means of cryoelectron microscopy and X-ray crystallography of virus-Fab complexes. J. Virol. *72*, 4610–4622.
8. Huang, M., et al., and Ruf, W. (1998). The mechanism of an inhibitory antibody on TF-initiated blood coagulation revealed by the crystal structures of human tissue factor, Fab 5G9 and TF.5G9 complex. J. Mol. Biol. *275*, 873–894.
9. Mylvaganam, S.E., Paterson, Y., and Getzoff, E.D. (1998). Structural basis for the binding of an anti-cytochrome c antibody to its antigen: crystal structures of FabE8-cytochrome c complex to 1.8 Å resolution and FabE8 to 2.26 Å resolution. J. Mol. Biol. *281*, 301–322.
10. Wilson, I.A., and Stanfield, R.L. (1993). Antibody-antigen interactions. Curr. Opin. Struct. Biol. *3*, 113–118.
11. Wilson, I.A., and Stanfield, R.L. (1994). Antibody-antigen interactions: new structures and new conformational changes. Curr. Opin. Struct. Biol. *4*, 857–867.
12. Davies, D.R., and Cohen, G.H. (1996). Interactions of protein antigens with antibodies. Proc. Natl. Acad. Sci. USA *93*, 7–12.
13. Bhat, T.N. Bentley, G.A., Fischmann, T.O., Boulot, G., and Poljak, R.J. (1990). Small rearrangements in structures of Fv and Fab fragments of antibody D1.3 on antigen binding. Nature *347*, 583–485.
14. Freed, E.O. (1998). HIV-1 Gag proteins: diverse functions in the virus life cycle. Virology *251*, 1–15.
15. Wilk, T., and Fuller, S.D. (1999). Towards the structure of the human immunodeficiency virus: divide and conquer. Curr. Opin. Struct. Biol. *9*, 231–243.
16. Janvier, B., et al., and Barin, F. (1993). Prevalence and persistence of antibody titers to recombinant HIV-1 core and matrix proteins in HIV-1 infection. J. Acquir. Immune Defic. Syndr. *6*, 898–903.
17. Chenet, V., Verrier, B., and Mallet, F. (1993). Over-expression of HIV-1 proteins in *Escherichia coli* by a modified expression vector and their one-step purification. Protein Expr. Purif. *4*, 367–372.
18. Berthet-Colominas, C., Monaco, S., Novelli, A., Sibaï, G., Mallet, F., and Cusack, S. (1999). Head-to-tail dimers and interdomain flexibility revealed by the crystal structure of HIV-1 capsid protein (p24) complexed with a monoclonal antibody Fab. EMBO J. *18*, 1124–1136.
19. Gamble, T.R., Yoo, S., Vajdos, F.F. Von Schwedler, UK, Worthylake D.K., Wang, H., McCutcheon, J.P., Sundquist, W.I., and Hill, C.P. (1997). Structure of the carboxyl-terminal dimerization domain of the HIV-1 capsid protein. Science *278*, 849–852.
20. Kabat, E.A., Wu, T.T., Perry, H.M., Gottesman, K.S., and Foeller, C. (1991). Sequences of Proteins of Immunological Interest, Fifteenth Edition (New York: US Department of Health and Human Services).
21. Milner-White, E.J., Ross, B.M., Ismail, R., Belhadj-Mostefa, K., and Poet, R. (1988). One type of gamma-turn, rather than the other gives rise to chain-reversal in proteins. J. Mol. Biol. *204*, 777–782.
22. Padlan, E.A. (1996). X-ray crystallography of antibodies. Adv. Protein Chem. *49*, 57–133.
23. Chothia, C., et al., and Poljak, R.J. (1989). Conformations of immunoglobulin hypervariable regions. Nature *342*, 877–883.
24. Gamble, T.R., et al., and Hill, C.P. (1996). Crystal structure of human cyclophilin A bound to the amino-terminal domain of HIV-1 capsid. Cell *87*, 1285–1294.
25. Worthylake, D.K., Wang, H., Yoo, S., Sundquist, W.I., and Hill, C.P. (1999). Structures of the HIV-1 capsid protein dimerization domain at 2.6 A resolution. Acta Crystollagr. D *55*, 85–92.
26. Stanfield, R.L., Takimoto-Kamimura, M., Rini, J.M., Profy, A.T., and Wilson, I.A. (1993). Major antigen-induced domain rearrangements in an antibody. Structure *1*, 83–93.
27. Zeder-Lutz, G., Zuber, E., Witz, J., and Van Regenmortel, M.H. (1997). Thermodynamic analysis of antigen-antibody binding using biosensor measurements at different temperatures. Anal. Biochem. *246*, 123–132.
28. Oddie, G.W., Gruen, L.C., Odgers, G.A., King, L.G., and Kortt, A.A. (1997). Identification and minimization of nonideal binding effects in BIAcore analysis: ferritin/anti-ferritin Fab' interaction as a model system. Anal. Biochem. *244*, 301–311.
29. Löfas, S., and Johnsson, B. (1990). A novel hydrogen matrix on gold surfaces in plasmon resonance sensors for fast and efficient covalent

immobilization of ligands. J. Chem. Soc. Chem. Commun. *21*, 1526–1528.
30. Fagerstam, L.G., et al., and Butt, H. (1990). Detection of antigen-antibody interactions by surface plasmon resonance. Application to epitope mapping. J. Mol. Recognit *3*, 208–214.
31. Matthews, B.W. (1968). Solvent content of protein crystals. J. Mol. Biol. *33*, 491–497.
32. Leslie, A.G.W. (1992). Joint CCP4 and ESF-EACBM Newsletter on Protein Crystallography, Number *26* (Warrington, UK: Daresbury Laboratory).
33. Colloborative Computational Project number 4. (1994). The CCP4 suite: programs for protein crystallography. Acta Crystallogr. D *50*, 760–763.
34. Navaza, J. (1994). Amore: an automated package for molecular replacement. Acta Crystallogr. A *50*, 157–163.
35. Momany, C., et al., and Rossmann, M.G. (1996). Crystal structure of dimeric HIV-1 capsid protein. Nat. Struct. Biol. *3*, 763–770.
36. Brünger, A.T., Krukowski, A., and Erickson, J. (1990). Slow-cooling protocols for crystallographic refinement by simulated annealing. Acta Crystallogr. A *46*, 585–593.
37. Jones, T.A., Zou, J.-Y., Cowan, S.W., and Kjeldgaard, M. (1991). Improved methods for building protein models in electron density maps and the location of errors in these models. Acta Crystallogr. A *47*, 110–199.
38. Kleywegt, G.J., and Jones, T.A. (1994). A super position. ESF/CCP4 Newsletter *31*, 9–14.
39. Laskowski, R.A., MacArthur, M.W., Moss, D.S., and Thornton, J.M. (1993). PROCHECK: a program to check the stereochemical quality of protein structures. J. Appl. Crystallogr. *26*, 283–291.

Protein Data Bank Coordinates

The Fab′13B5 coordinates have been deposited in the Protein Data Bank under the code 1e6o and the Fab-p24 complex with code 1e6j.